Available online at www.sciencedirect.com
ScienceDirect
Journal of the European Ceramic Society 28 (2008) 377–382
www.elsevier.com/locate/jeurceramsoc

Activation energy of mullitization from various starting materials

Kiyoshi Okada *

Department of Metallurgy and Ceramics Science, Tokyo Institute of Technology, O-okayama, Meguro, Tokyo 152-8552, Japan

Available online 5 April 2007

Abstract

The activation energy (E_a) of mullitization from various starting materials was investigated using both our own data and data from the literature. The starting materials included mixtures of kaolinite and alumina, sol mixtures, diphasic gels, hybrid gels, monophasic gels, glasses and glass fibers. The first crystalline phase formed by heating these starting materials can be of two types, i.e. (1) γ-Al_2O_3, which is formed in mixtures of kaolinite and alumina, sol mixtures, diphasic gels and hybrid gels and (2) Al-rich mullite, formed in monophasic gels, glasses and glass fibers. Irrespective of the initial crystalline phase, the E_a values for mullitization range from 800 to 1400 kJ/mol and show a maximum at about 1000 °C. These E_a values are higher than for other silicates, for example, <800 kJ/mol found for the CaO–Al_2O_3–SiO_2 system, and are thought to be due to the overlap of the E_a values for nucleation and nucleation-growth (crystallization). The E_a values for both these processes are high for mullitization, reflecting the high E_a value for diffusion of Si ions in the Al_2O_3–SiO_2 system. The steps controlling mullitization in type (1) starting materials are thought to change at higher temperatures from being dominated by the transfer of alumina from γ-Al_2O_3 to amorphous silica, to diffusion-controlled processes. By contrast, reactions in type (2) starting materials proceed in three stages, nucleation, nucleation-growth and coalescence, as the heating temperature increases.

Keywords: Mullitization; Glass

1. Introduction

Mullite ($Al_{4+2x}Si_{2-2x}O_{10-x}$) can be prepared from a variety of starting materials, all of which follow more or less different mullitization routes on heating. These pathways fall into two broad categories, i.e. (1) mullite formation above 1200 °C via an γ-Al_2O_3 precursor, and (2) direct formation of Al-rich mullite at about 900–1000 °C.[1] The former behavior is observed in mixtures of kaolinite and alumina, sol mixtures and diphasic (colloidal) gels while the latter type is observed in monophasic (polymeric) gels and glasses. The main reason for the different mullitization routes is attributed to the different degree of mixing of the Al_2O_3 and SiO_2 in the grains and on a molecular scale, respectively.

Many researchers have also investigated the kinetics of mullitization, all reporting that mullitization occurs by nucleation-growth mechanisms. There are, however, different opinions on the rate-controlling step of mullitization, listed in Table 1. Wei and Halloran[2] investigated the mullitization kinetics of a diphasic gel (type (1)) and proposed a mechanism involving either interface-control or control by short-range diffusion near the interface. Hulling and Messing[5] considered that release of alumina from the initially-formed γ-Al_2O_3 structure is the rate-controlling step in mullitization from diphasic and hybrid gels. Sundaresan and Aksay[6] reported a similar rate-limiting mechanism for the growth of mullite nuclei in the mullitization of a diphasic gel, and also suggested that mullitization is limited by alumina dissolution (release) at low temperatures (<1350 °C), but by diffusion at high temperatures (<1650 °C). Based on this model, the E_a for diffusion in the amorphous aluminosilicate matrix must be smaller than that of alumina released from the γ-Al_2O_3 structure in type (1) starting materials.

As pointed out above, the rate-controlling step of mullitization has been well investigated for starting materials of type (1) but little work has been reported on the controlling step of mullitization from type (2) starting materials. The first paper on this topic was by Li and Thomson,[3] who made high-temperature XRD in situ measurements and suggested that the rate-controlling step for mullitization from monophasic gels (type (2)) is nucleation controlled. However, their reported E_a values of 293 ± 145 and 362 ± 145 kJ/mol are smaller than the other reported data listed in Table 1.[1–16] Takei et al.[10] found that mullitization from glass fibers can be kinematically divided into three

* Tel.: +81 3 5734 2524; fax: +81 3 5734 3355.
E-mail address: kokada@ceram.titech.ac.jp.

0955-2219/$ – see front matter © 2007 Elsevier Ltd. All rights reserved.
doi:10.1016/j.jeurceramsoc.2007.03.015

Table 1
Activation energies and mechanisms of mullitization reported by many authors

Authors	Starting materials	Al_2O_3 (mol%)	1st crystalline phase	E_{NG} (kJ/mol)	Temperature range (°C)	Method	Controlling step
Wei and Halloran[2]	Diphasic gel	60	γ-Al_2O_3	1070(200)	1200–1300	XRD	Interface
Li and Thomson[3]	Monophasic gel	60	Mullite	293(145)	940–1040	HT-XRD	Nucleation
Li and Thomson[3]	Monophasic gel	60	Mullite	362(145)	940–1040	HT-XRD	Nucleation
Li and Thomson[4]	Diphasic gel	60	γ-Al_2O_3	1034(37)	1300–1390	DTA	–
Li and Thomson[4]	Diphasic gel	60.8	γ-Al_2O_3	1108(44)	1300–1390	DTA	–
Hulling and Messing[5]	Hybrid gel	58.6	γ-Al_2O_3	932(49)	1200–1275	XRD	Al release
Hulling and Messing[5]	Hybrid gel	60	γ-Al_2O_3	960(91)	1200–1275	XRD	Al release
Hulling and Messing[5]	Hybrid gel	61.4	γ-Al_2O_3	984(71)	1200–1275	XRD	Al release
Hulling and Messing[5]	Hybrid gel	61.4	γ-Al_2O_3	1091(71)	1200–1275	XRD	Al release
Sundaresan and Aksay[6]	Diphasic gel	60	γ-Al_2O_3	–	–	–	Al dissolution
Lee and Yu[7]	Coprecipitated gel	59.7	γ-Al_2O_3	891(17)	1275–1315	DTA	–
Lee and Yu[7]	Coprecipitated gel	59.8	γ-Al_2O_3	829(24)	1265–1310	DTA	–
Lee and Yu[7]	Coprecipitated gel	60.3	γ-Al_2O_3	759(26)	1255–1300	DTA	–
Lee and Yu[7]	Coprecipitated gel	60.4	γ-Al_2O_3	841(23)	1275–1315	DTA	–
Lee and Yu[7]	Coprecipitated gel	62.5	γ-Al_2O_3	860(32)	1275–1315	DTA	–
Tkalcec et al.[8]	Monophasic gel	60	Mullite	1053(51)	937–959	DSC	Phase separation
Boccaccini et al.[9]	Sol mix	60	γ-Al_2O_3	–	–	–	–
Takei et al.[10]	Glass fiber	56.7	Mullite	1138(29)	920–965	XRD	Three different steps
Johnson et al.[11]	Glass	60	Mullite	892	946–971	DSC	–
Okada et al.[12]	Monophasic gel	60	Mullite	1202(27)	969–998	DTA	Diffusion
Chen et al.[13]	Kaolinite + Al_2O_3	60	Mullite	1357	1000–1300	XRD	–
Chen et al.[13]	Kaolinite + Al_2O_3	60	Mullite	1165	1300–1600	XRD	–
Chen et al.[14]	Kaolinite + Al_2O_3	60	Mullite	1182	1006–1022	DTA	Diffusion
Tkalcec et al.[15]	Diphasic gel	60	γ-Al_2O_3	935(14)	1219–1251	DSC	–
Tkalcec et al.[15]	Diphasic gel	60	Mullite	1119(25)	1248–1275	DSC	–
Douy[16]	Monophasic gel	60	Mullite	1395(145)	973	DSC	–

parts; based on their mullitization curve and observed changes in grain size, thy identified the following processes: nucleation at low temperatures (920–965 °C), nucleation-growth at intermediate temperatures (965–1200 °C) and coalescence of mullite grains at high temperatures (≥1200 °C). The major rate-controlling steps for nucleation and nucleation-growth were thought to be diffusion of Si ions in the amorphous matrix.

In this paper, we summarize the E_a values for mullitization from various starting materials determined by us and by other researchers, and discuss the reasons for the unusually large E_a values for mullitization.

2. Experiments and calculations of the activation energy of mullitization

The activation energy (E_a) of mullitization has been determined by various methods using both powders and bulk samples. The experiments may be made under either isothermal or non-isothermal conditions. Powder samples are usually investigated by isothermal experiments, by the analysis of XRD data for samples heated at various temperatures and times (but Li and Thomson[3] used in situ high temperature XRD to obtain their E_a values). The crystallization rate in bulk samples can be obtained by measuring the thickness of the crystallized layer by SEM in the case of surface crystallization. This method is however difficult to adapt to the Al_2O_3–SiO_2 system because ultra-rapid quenching is necessary to obtain a glassy state in mullite compositions, suggesting that it is nearly impossible to obtain a bulk sample.

Under isothermal conditions, the E_a values for nucleation can be deduced from the temperature dependence of the incubation time (τ) of the mullitization curves. The E_a values for nucleation (E_a^N) can be calculated from Eq. (1):

$$\tau = \tau_0 \exp\left(\frac{E_a^N}{RT}\right) \quad (1)$$

where τ_0 is a constant, R the gas constant and T is the absolute temperature. The value of τ is generally determined from the time at which the volume fraction of crystallized mullite comprises 2 vol% of the sample. After obtaining an isothermal mullitization curve as a function of heating time it is necessary to mathematically fit the data using equations for the various possible kinetic mechanisms (diffusion controlled, phase-boundary controlled or nucleation-growth). Although the mathematical equations have been reported for all these kinetic mechanisms,[17] not all the reports examine the mechanistic implications in detail, but merely adopt a nucleation-growth mechanism for mullitization based on the kinetic curve shape. Thus, the well-known Avrami equation is used for the curve fitting, the rate of nucleation-growth (k) being obtained from Eq. (2) and the E_a value for nucleation-growth (E_a^{NG}) calculated using Eq. (3):

$$1 - x = \exp[-(kt)^n] \quad (2)$$

$$k = k_0 \exp\left[-\left(\frac{E_a^{NG}}{RT}\right)\right] \quad (3)$$

where x is the volume fraction of crystallized mullite, t the heating time, n an Avrami dimension and k_0 is a constant.

Under non-isothermal conditions, DTA or DSC curves are used to obtain E_a values from peak temperature measurements at different heating rates. Although many mathematical equations have been proposed for the calculations, the Kissinger equation[18] (Eq. (4)) is most commonly used.

$$\ln\left(\frac{T_p^2}{\phi}\right) = \ln\left(\frac{E_a}{R}\right) - \ln\nu + \frac{E_a}{(RT_p)} \quad (4)$$

where T_p is the temperature of the exothermic peak top (crystallization temperature), ϕ the heating rate and ν is the frequency factor. A non-isothermal method is experimentally easier than an isothermal method, but the accuracy of the resulting E_a value is generally lower than for values determined by isothermal methods, for the following reasons: the crystallization peak becomes weaker and broader at slower heating rates, limiting the plotting range of $(1/T_p)$. This is in addition to instrumental limitations which prevent the slope value corresponding to E_a from being determined accurately. Furthermore, T_p values are generally strongly influenced by experimental conditions such as particle size, particle distribution, packing state, etc.

3. Activation energy of nucleation of mullite

The E_a values for the nucleation of mullite (E_a^N) were obtained using incubation time data (Eq. (1)) for a diphasic gel by Wei and Halloran[2] and for glass fibers by Takei et al.[10] The diphasic gel follows a type (1) mullitization route while the glass fibers follow type (2). The E_a^N value for the diphasic gel with $Al_2O_3 = 60$ mol% at 1200–1300 °C is 987 ± 63 kJ/mol. Since the mixing of the Al_2O_3 and SiO_2 in this starting material is not on the molecular scale, but occurs at the level of the grains, interdiffusion of Al_2O_3 and SiO_2, even over a short distance, is necessary for the formation of mullite nuclei in the sample, and is suggested to be the predominant rate-controlling step for nucleation of mullite in diphasic gels. Although the large E_a^N value is suggested to be due to the low diffusitivity of Si ion, the predominant rate-controlling step for nucleation-growth of mullite from a diphasic gel was thought to be either the release of alumina from γ-Al_2O_3 grains (Hulling and Messing[5]) or Al dissolution (Sundaresan and Aksay[6]).

On the other hand, the E_a^N values for glass fibers with $Al_2O_3 = 36.1$ and 56.7 mol% obtained at 920–965 °C are 864 ± 65 and 980 ± 52 kJ/mol, respectively. Since the former glass fibers are richer in SiO_2 than mullite, interdiffusion of Al_2O_3 and SiO_2 is necessary to form mullite nuclei in the glass matrix, assuming the glass fibers are homogeneous. By contrast, the glass fibers with $Al_2O_3 = 56.7$ mol% have a closely similar chemical composition to mullite. Thus, mullite nuclei can be formed without interdiffusion of Al_2O_3 and SiO_2 in this sample and the resulting E_a^N values should be lower than in the former glass fibers for this reason. However, the measured E_a^N values are rather lower in the former glass fibers than in the latter. This may be due to the metastable phase separation reported in the Al_2O_3–SiO_2 system by many researchers. These unexpected E_a^N results may be influenced by this phase separation which will form interfaces thermo-energetically more favorable as heterogeneous nucleation sites for mullitization in the glass matrix. This will be discussed further in Section 4.2.

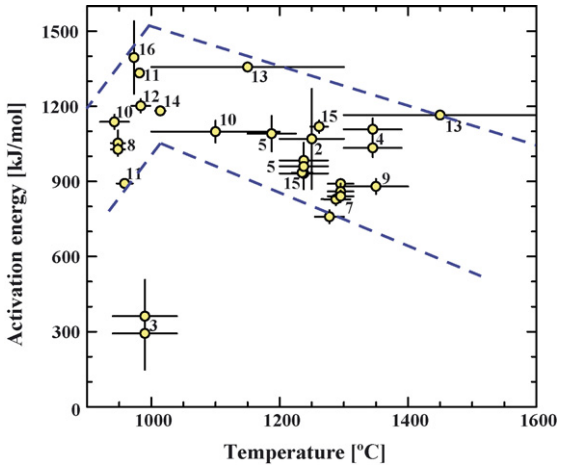

Fig. 1. Relationship between E_a of mullitization and the temperature range in which the E_a values for the various starting materials are derived. The vertical lines are error bars of E_a. The figures represent reference numbers.

4. Activation energy of nucleation-growth of mullite

4.1. Activation energy and mullitization temperature

Fig. 1[1–16] shows the relationship between E_a for nucleation-growth of mullite (E_a^{NG}) and the temperature range in which the E_a values for the various starting materials were derived. Although the data show considerable scatter, a trend with temperature is shown by the broken lines, except for the data of Ref. 3. This trend is to increased E_a with increasing temperature in the range ≤1000 °C, but decreasing E_a at higher temperatures (>1000 °C). Since direct mullitization from an amorphous phase occurs in the low temperature range (900–1000 °C), the increasing trend of E_a corresponds to formation of Al-rich mullite. In this case, Al_2O_3 and SiO_2 are thought to be molecularly well mixed in amorphous type (2) starting materials. Thus, only atomic re-arrangements within short- to middle-range distances are sufficient to form mullite nuclei in the amorphous matrix, and nucleation should be the dominant rate-controlling step for the mullitization. The E_a values for nucleation-growth controlled mullitization (900–1400 kJ/mol) are a little higher than the E_a^N values obtained from incubation time data and are distinctly larger than E_a for nucleation of other crystalline phases.

The E_a values of mullitization were therefore compared with those for the nucleation of various crystalline phases from glasses and amorphous phases in the alkaline earth aluminosilicates and alkali (-alkaline earth) silicates. These E_a values are plotted in Fig. 2[19–34] as a function of crystallization temperature. A trend to increasing E_a with increasing crystallization temperature is clearly observed. The E_a values for mullitization deviate distinctly from this relationship, occurring at higher E_a values. This suggests that the ion mobilities in the amorphous Al_2O_3–SiO_2 phases are lower than in alkaline earth aluminosilicates and alkali (-alkaline earth) silicates, resulting in higher E_a values because of the lack of framework modifiers of alkali

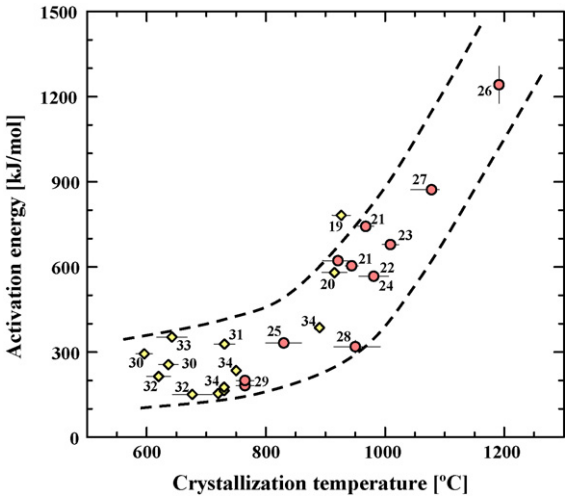

Fig. 2. Relationship between E_a and the crystallization temperature of various alkaline and alkaline earth silicates (rhombuses) and aluminosilicates (circles). The vertical and horizontal lines are error bars of E_a and temperature ranges in which the E_a values for the various starting materials are derived. The figures represent reference numbers.

and/or alkaline earth ions in the amorphous Al_2O_3–SiO_2 phases. This interpretation can reasonably explain the large difference of E_a values in the above crystallization reactions, but is inapplicable to the SiO_2 phase; the E_a values reported for crystallization of cristobalite from amorphous silica with no framework modifiers are only several 100 kJ/mol.[17] Other factors must also be operating to produce the large E_a values for nucleation-growth in mullitization.

In the higher temperature range (>1000 °C), the E_a values decrease slightly with increasing mullitization temperature. A similar temperature dependency is also observed in the E_a values of various crystalline phases in the CaO–Al_2O_3–SiO_2 system (Fig. 3).[1–16,19–24,35–37] As pointed out by Sundaresan and Aksay[6] for type (1) starting materials, diffusion becomes more

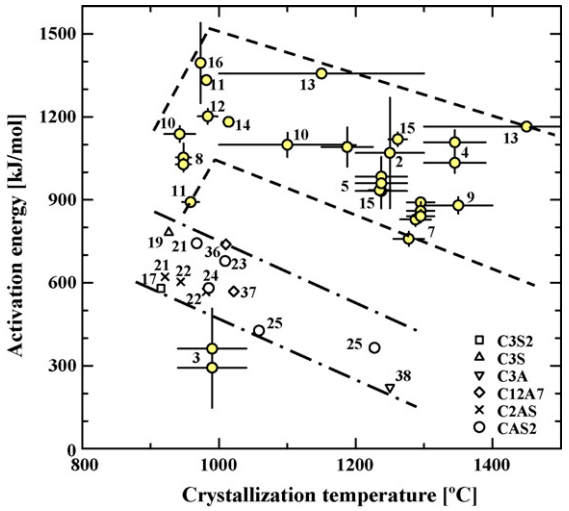

Fig. 3. Comparison of relationships between E_a of crystallization and temperature range in which the E_a values for the various starting materials are derived in the CaO–Al_2O_3–SiO_2 system and mullite. The vertical lines are error bars of E_a. The figures represent reference numbers.

Table 2
Comparison of diffusion coefficient (D_0) and activation energy (Q) values for diffusion coefficient of Si^{4+}

Sample	Composition (mol%)			D_0 (cm^2/s)	Q (kJ/mol)	Reference
	CaO	Al_2O_3	SiO_2			
Mullite	0	60	40	3.23×10^3	703	38
Mullite	0	60	40	–	714	39
Mullite	0	60	40	–	803	40
Mullite	0	60	40	7.01×10^4	730	41
Mullite	0	60	40	3.37×10^5	781	41
CAS melt	45.3	12.4	42.3	1.25×10^3	329	42

dominant as the rate-controlling step at increasing higher mullitization temperatures. Thus, the dominant kinetic mechanism changes from nucleation to growth and the rate-controlling step changes from the release of alumina in type (1) starting materials and from nucleation control in type (2) to diffusion controlled at higher mullitization temperatures. In the Al_2O_3–SiO_2 system, diffusion of Si is clearly slower than that of Al or O, and becomes the rate-controlling step for mullitization at high temperatures. The reported data for Si diffusion in the Al_2O_3–SiO_2 system are listed in Table 2[38–42] together with data for the CaO–Al_2O_3–SiO_2 system. The reported E_a values for Si diffusion (700–800 kJ/mol) are clearly lower than the observed E_a values for mullitization (nucleation controlled) at low temperatures, they become more comparable with the E_a values at high temperatures (diffusion controlled) (Fig. 1). As pointed out by Takei et al.,[10] further growth of mullite causes coalescence of the grains, with an E_a (600–700 kJ/mol) a little lower than for Si diffusion. The controlling step for this stage is thus grain boundary reaction. Table 2 shows that the E_a values for Si diffusion in the Al_2O_3–SiO_2 system are more than double those for the CaO–Al_2O_3–SiO_2 system.[42] The differences are suggested to strongly influence the E_a values of the various types of crystallization.

The temperature dependence of the E_a values of mullitization suggests that the dominant kinetic mechanism changes from nucleation → growth → coalescence with increasing mullitization temperature, and the corresponding dominant rate-controlling steps are the generation of nuclei by the release of alumina from γ-alumina to amorphous silica (in type (1) starting materials) or by structural re-arrangement (in type (2) materials). The suggested progression of rate-controlling steps is then: generation of nuclei → Si diffusion (growth of nucleated particles and mullite grains) → grain boundary reaction (grain growth by coalescence).

4.2. Activation energy and chemical composition

Douy[16] has recently reported a systematic examination of E_a for mullitization at low temperature (near 1000 °C) from monophasic gels of varying chemical composition. These and corresponding data, plotted in Fig. 4[10,12,16,17] as a function of the Al_2O_3 content (mol%) in the starting materials, show a maximum value of E_a at the mullite composition. The decrease of E_a in more Al_2O_3–rich compositions is thought to be due to

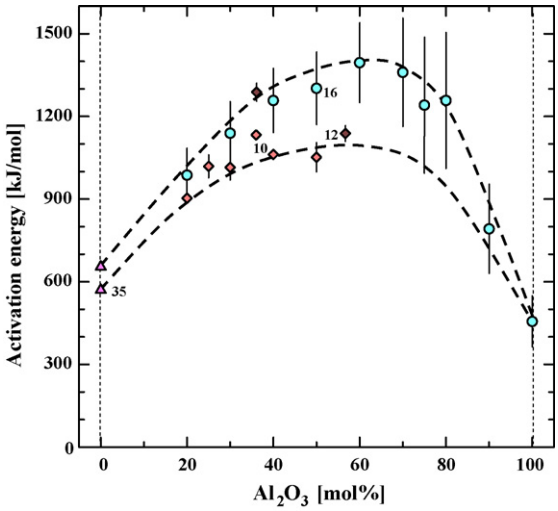

Fig. 4. Relationship between E_a and Al_2O_3 content of the starting materials in the SiO_2–Al_2O_3 system. The vertical lines are error bars of E_a. The figures represent reference numbers.

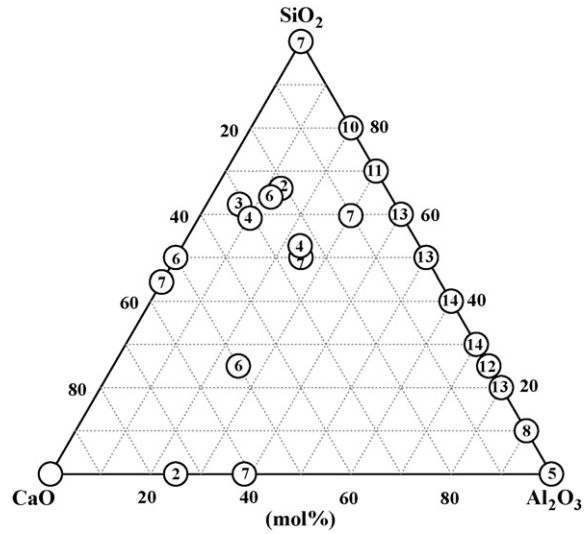

Fig. 5. Relationship between E_a ($\times 10^2$ kJ/mol) and chemical composition of the starting materials in the CaO–Al_2O_3–SiO_2 system.

the simultaneous crystallization of mullite and γ-Al_2O_3, the latter having a lower E_a than mullite, and thereby lowering the arithmetic average of the resulting E_a values. By contrast, the E_a values decrease with increasing SiO_2 content above the mullite composition, even though the crystalline phase is only mullite and does not contain cristobalite. A possible explanation of this result may be the effect of interfaces introduced by phase separation occurring prior to crystallization.[43] Based on the calculated phase separated region, ordinary mullite composition corresponds to the nucleation-growth region (bimodal) and the microstructure forms a particulate structure containing particles of SiO_2-rich composition dispersed in a matrix of Al-rich mullite composition. Thus, the ratio of the interface area (containing preferable heterogeneous nucleation sites) to the volume of the Al-rich mullite composition region, is rather low in this microstructure. With starting materials of higher SiO_2 content, the phase-separated microstructure changes to a spinodal-type, consisting of two continuous regions with SiO_2-rich and Al-rich mullite compositions, and then to a nucleation-growth region with a particulate structure of dispersed particles of Al-rich mullite composition in a matrix of SiO_2-rich composition. Both these microstructure changes and the increase of the interface-to-volume ratio of the region of Al-rich mullite composition, have the effect of lowering the thermodynamic barrier for nucleation of mullite from the interface to the inside of the region of Al-rich mullite composition, resulting in lower E_a values.

As mentioned in Section 4.1, we are not fully able to explain the high E_a values of mullitization, which are clearly greater than those of the various crystalline phases in the CaO–Al_2O_3–SiO_2 system (Fig. 5). There are two possible reasons for these differences. In calcium containing glasses, the glass transition temperatures (T_g) are always >100–200 °C lower than the corresponding crystallization temperatures (T_c), i.e. the exothermic peak temperature in the DTA curve.[44] Since the nucleation temperature is generally lower than or close to T_g, the thermodynamic barriers for nucleation and crystallization (growth > nucleation) are clearly separated in these glasses. By contrast, the T_g values of Al_2O_3–SiO_2 glasses are much closer to T_c (within 50 °C).[16] We therefore consider that the thermodynamic and kinematic barriers to nucleation and crystallization (growth > nucleation) overlap in the Al_2O_3–SiO_2 glasses, giving E_a values which are larger than in the CaO–Al_2O_3–SiO_2 glasses. A second possible reason is the stronger bonding energy of Si–O and Al–O compared with Ca–O, presenting a higher thermodynamic barrier to the crystallization of mullite, a process involving the re-arrangement of the short- to medium-range structure.

5. Summary

The activation energies (E_a) reported for mullitization from various starting materials were summarized with respect to nucleation and nucleation-growth mechanisms. The dependence of E_a for mullite nucleation-growth on the mullitization temperature and chemical composition of the starting materials was also investigated.

The E_a values of mullite nucleation (E_a^N) obtained from diphasic gel (type (1) starting material) and glass fibers (type (2) starting material), calculated from Eq. (1) were 800–1000 kJ/mol. These values are very similar, even though the rate-controlling steps of their nucleation are different, i.e. the release of alumina from γ-Al_2O_3 to amorphous silica, and nucleation, respectively.

Interfaces introduced by phase separation of amorphous Al_2O_3–SiO_2 which occurs prior to mullitization affects the E_a values of nucleation in the type (2) starting materials.

The E_a values for nucleation-growth of mullite obtained from various starting materials reach a maximum of about 1400 kJ/mol at about 1000 °C. Since the mullite formed in this temperature range is from type (2) starting material, this mullitization occurs by formation of mullite nuclei from an amorphous phase, i.e. nucleation is the controlling step. The E_a values for nucleation obtained from mullitization rate constants calculated from Eqs. (3) and (4) are slightly higher than those derived from incubation times, calculated from Eq. (1). At mullitiza-

tion temperatures >1000 °C, the controlling step becomes more predominantly diffusion, especially of Si ions. At even higher temperatures, coalescence of mullite grains is the dominant rate-controlling step.

The very high E_a values of nucleation and nucleation-growth of mullite are attributed to a combination of reasons such as the overlap of thermodynamic and kinematic barriers for nucleation and crystallization (E_a^N and E_a^{NG}), low mobility of ions (low viscosity) in the amorphous state and slow diffusion of Si ions in the Al_2O_3–SiO_2 system.

Acknowledgement

We are grateful to Professor K.J.D. MacKenzie of Victoria University of Wellington for critical reading and editing of the manuscript.

References

1. Okada, K., Otsuka, N. and Somiya, S., Review of mullite synthesis routes in Japan. *Am. Ceram. Soc. Bull.*, 1991, **70**(10), 1633–1640.
2. Wei, W.-C. and Halloran, J. W., Transformation kinetics of diphasic aluminosilicate gels. *J. Am. Ceram. Soc.*, 1988, **71**(7), 581–587.
3. Li, D. X. and Thomson, W. J., Mullite formation kinetics of a single-phase gel. *J. Am. Ceram. Soc.*, 1990, **73**(4), 964–969.
4. Li, D. X. and Thomson, W. J., Mullite formation from nonstoichiometric diphasic precursors. *J. Am. Ceram. Soc.*, 1991, **74**(10), 2382–2387.
5. Hulling, J. C. and Messing, G. L., Epitactic nucleation of spinel in aluminosilicate gels and its effect on mullite crystallization. *J. Am. Ceram. Soc.*, 1991, **74**(10), 2374–2381.
6. Sundaresan, S. and Aksay, I. A., Mullitization of diphasic aluminosilicate gels. *J. Am. Ceram. Soc.*, 1991, **74**(10), 2388–2392.
7. Lee, J.-S. and Yu, S.-C., Mullite formation kinetics of coprecipitated Al_2O_3–SiO_2 gels. *Mater. Res. Bull.*, 1992, **27**(4), 405–416.
8. Tkalcec, E., Nass, R., Schmauch, J., Schmidt, H., Kurajica, S., Bezjak, A. *et al.*, Crystallization kinetics of mullite from single-phase gel determined by isothermal differential scanning calorimetry. *J. Non-Cryst. Solids*, 1998, **223**(1), 57–72.
9. Boccaccini, A. R., Khalil, T. K. and Bucker, M., Activation energy for the mullitization of a diphasic gel obtained from fumed silica and boehmite sol. *Mater. Lett.*, 1999, **38**(2), 116–120.
10. Takei, T., Kameshima, Y., Yasumori, A. and Okada, K., Crystallization kinetics of mullite in alumina–silica glass fibers. *J. Am. Ceram. Soc.*, 1999, **82**(10), 2876–2880.
11. Johnson, B. R., Kriven, W. M. and Schneider, J., Crystal structure development during devitrification of quenched mullite. *J. Eur. Ceram. Soc.*, 2001, **21**(14), 2541–2562.
12. Okada, K., Kaneda, J., Kameshima, Y., Yasumori, A. and Takei, T., Crystallization kinetics of mullite from polymeric Al_2O_3–SiO_2 xerogels. *Mater. Res. Bull.*, 2003, **57**(21), 3155–3159.
13. Chen, Y.-F., Wang, M.-C. and Hon, M.-H., Transformation kinetics for mullite in kaolin-Al_2O_3 ceramics. *J. Mater. Res.*, 2003, **18**(6), 1355–1362.
14. Chen, Y.-F., Wang, M.-C. and Hon, M.-H., Phase transformation and growth of mullite in kaolin ceramics. *J. Eur. Ceram. Soc.*, 2004, **24**(8), 2389–2397.
15. Tkalcec, E., Kurajica, S. and Ivankovic, H., Diphasic aluminosilicate gels with two stage mullitization in temperature range of 1200–1300 °C. *J. Eur. Ceram. Soc.*, 2005, **25**(5), 613–626.
16. Douy, A., Crystallization of amorphous spray-dried precursors in the Al_2O_3–SiO_2 system. *J. Eur. Ceram. Soc.*, 2006, **26**(8), 1447–1454.
17. Wang, L. H. and Tsai, B. J., The sintering and crystallization of colloidal silica gel. *Mater. Lett.*, 2000, **43**(5/6), 309–314.
18. Kissinger, H. E., Reaction kinetics in differential thermal analysis. *Anal. Chem.*, 1957, **29**(9), 1702–1706.
19. Fan, X., Wang, M., Hong, Z. and Qian, G., The process of crystallization of $CaSiO_3$ gel and the luminescence of Eu^{3+} ions in gel-derived crystals. *J. Phys. Condensed Matter*, 1997, **9**(16), 3479–3486.
20. Laudisio, G., Catauro, M., Costantini, A. and Branda, F., Sol–gel preparation and crystallization of $2.5CaO{\cdot}2SiO_2$ glassy powders. *Thermochim. Acta*, 1998, **322**(1), 17–23.
21. Traore, K., Kabre, T. S. and Blanchart, P., Gehlenite and anorthite crystallization from kaolinite and calcite mix. *Ceram. Int.*, 2003, **29**(4), 377–383.
22. Marotta, A., Buri, A. and Valenti, G. L., Crystallization kinetics of gehlenite glass. *J. Mater. Sci.*, 1978, **13**(11), 2483–2486.
23. Park, H.-C., Lee, S.-H., Ryu, K., Son, M.-M., Lee, H.-S. and Yasui, I., Nucleation and crystallization kinetics of CaO–Al_2O_3–SiO_2. *J. Mater. Sci.*, 1996, **31**(16), 4249–4253.
24. Duan, R. G., Liang, K. M. and Gu, S. R., A study on the mechanism of crystal growth in the process of crystallization. *Mater. Res. Bull.*, 1998, **33**(8), 1143–1149.
25. Cheng, K., Determining crystallization kinetic parameters of Li_2O–Al_2O_3–SiO_2 glass from derivative differential analysis curves. *Mater. Sci. Eng.*, 1999, **B60**(3), 194–199.
26. Rocherulle, J. and Marchand, T., Nonisothermal devitrification study of an aluminosilicate glass matrix. *Mater. Res. Bull.*, 2000, **35**(1), 9–14.
27. Petrovic, R., Janakovic, D., Zec, S., Dramanic, S. and Gvozdenovic, K., Phase-transformation kinetics in triphasic cordierite gel. *J. Mater. Res.*, 2001, **16**(2), 451–458.
28. Sung, Y.-M., The effect of additives on the crystallization and sintering of $2MgO$–$2Al_2O_3$–$5SiO_2$. *J. Mater. Sci.*, 1996, **31**(20), 5421–5427.
29. Tosic, M. B., Mitrovic, M. M. and Dimitrijevic, R. Z., Crystallization of leucite as the main phase in aluminosilicate glass with low fluorine content. *J. Mater. Sci.*, 2000, **35**(14), 3659–3667.
30. Marotta, A., Buri, A. and Branda, F., Surface and bulk crystallization in non-isothermal devitrification of glasses. *Thermochim. Acta*, 1980, **40**(3), 397–403.
31. Marotta, A., Saiello, S., Branda, F. and Buri, A., Nucleation and crystal growth in $Na_2O{\cdot}2CaO{\cdot}3SiO_2$ glass. *Thermochim. Acta*, 1981, **46**(2), 123–129.
32. Branda, F., Buri, A., Marotta, A. and Saiello, S., Kinetics of crystal growth in $Na_2O{\cdot}2SiO_2$ glass. *Thermochim. Acta*, 1984, **77**(1–3), 13–18.
33. Branda, F., Buri, A. and Marotta, A., Nucleation and crystal growth in $0.9Li_2O{\cdot}0.1BaO{\cdot}2SiO_2$ glass. *Thermochim. Acta*, 1987, **120**(2), 217–223.
34. Branda, F., Buri, A., Marotta, A. and Saiello, S., Glass transition temperature and devitrification behavior of glasses in the $Na_2O{\cdot}2SiO_2$–$BaO{\cdot}2SiO_2$ composition range. *J. Mater. Sci. Lett.*, 1984, **3**(7), 654–658.
35. Li, W. and Mitchell, B. S., Nucleation and crystallization in calcium aluminate glasses. *J. Non-Cryst. Solids*, 1999, **255**(2–3), 199–207.
36. Sung, Y.-M. and Sung, J.-H., Crystallization behaviour of calcium aluminate glass fibers. *J. Mater. Sci.*, 1998, **33**(19), 4733–4737.
37. Mohamed, B. M. and Sharp, J. H., Kinetics and mechanism of formation of tricalcium aluminate, $Ca_3Al_2O_6$. *Thermochim. Acta*, 2002, **388**(2), 105–114.
38. Aksay, I. A. and Pask, J. A., Stable and metastable equilibria in the system SiO_2–Al_2O_3. *J. Am. Ceram. Soc.*, 1975, **58**(11-12), 507–512.
39. Dokko, P. C., Pask, J. A. and Mazdiyasni, K. S., High-temperature mechanical properties of mullite under compression. *J. Am. Ceram. Soc.*, 1977, **60**(3/4), 150–155.
40. Hynes, A. P. and Doremus, R. H., High-temperature compressive creep of polycrystalline mullite. *J. Am. Ceram. Soc.*, 1991, **74**(10–12), 2469–2475.
41. Sung, Y.-M., Determination of interdiffusion coefficient of mullite formation reaction via kinetics analysis. *J. Mater. Sci. Lett.*, 2001, **20**(15), 1433–1434.
42. Oishi, Y. and Nanba, M., Analysis of liquid-state interdiffusion the system CaO–Al_2O_3–SiO_2 using multiatomic ion models. *J. Am. Ceram. Soc.*, 1982, **65**(1), 247–253.
43. Takei, T., Kameshima, Y., Yasumori, A. and Okada, K., Calculation of metastable immiscibility region in the Al_2O_3–SiO_2 system using molecular dynamics simulation. *J. Mater. Res.*, 2000, **15**(1), 186–193.
44. Toya, T., Kameshima, Y., Yasumori, A. and Okada, K., Preparation and properties of glass-ceramics from wastes (Kira) of silica sand and kaolin clay refining. *J. Eur. Ceram. Soc.*, 2004, **24**(8), 2367–2372.